TABLE I. *MLL2* and *KDM6A* Mutations in Patients With KS

Patient ID	Method	Mutation	Predicted amino acid change	De novo	Remarks[a]
Patients with *MLL2* mutations					
KMS-02	H	c.9831_9848dup	p.Gln3277_Gln3282dup	Unknown	Novel
KMS-08	H	c.12688C > T	p.Gln4230*	Yes	Hannibal et al. [2011]
KMS-13	H	c.2433_2434insCA	p.Glu812Glnfs*119	Yes	Novel
KMS-14	H	c.11806_11807dup	p. Gln3936Hisfs*44	Yes	Novel
KMS-15	H	c.15119A > G	p.Asp5040Gly	Yes	Novel
KMS-17	H	c.5707C > T	p.Arg1903*	Yes	Novel
KMS-18	W	c.12151delA	p.Ile4051*	Yes	Novel
KMS-20	H	c.1300delC	p.Leu434*	Unknown	Novel
KMS-21	W	c.3326_3336dup	p.Asp1113Profs*10	Unknown	Novel
KMS-22	H	c.4127T > G	p.Met1376Arg	Unknown	Novel
KMS-23	W	c.15461G > A	p.Arg5154Gln	Unknown	Li et al. [2011]
KMS-24	H	c.2608 G > T	p.Glu870*	Unknown	Novel
KMS-25	H	c.11917C > T	p.Gln3973*	Unknown	Novel
KMS-27	H	c.15142C > T	p.Arg5048Cys	Yes	Hannibal et al. [2011], Makrythanasis et al. [2013]
KMS-28	H	c.14861C > A	p.Ser4954*	Unknown	Novel
KMS-29	H	c.4419-1G > T	splice site	Unknown	Novel
KMS-30	H	c.4633C > T	p. Gln1545*	Unknown	Novel
KMS-32	H	c.8059C > T	p.Arg2687*	Unknown	Banka et al. [2012b]
KMS-33	T	c.11962C > T	p.Gln3988*	Unknown	Novel
KMS-36	H	c.4736_4737delAG	p.Glu1579Alafs*23	Unknown	Novel
KMS-38	H	c.15143G > A	p.Arg5048His	Unknown	Makrythanasis et al. [2013]
KMS-40	T	c.15163_15168dup	p.Asp5055_Leu5056dup	Unknown	Micale et al. [2011]
KMS-41	H	c.1328delC	p.Pro443Hisfs*487	Yes	Ng et al. [2010]
KMS-42	H	c.16052G > A	p.Arg5351Gln	Yes	Novel
KMS-43	H	c.510 + 1G > A	splice site	Unknown	Novel
KMS-49	T	c.15565G > A	p.Gly5189Arg	Unknown	Novel
KMS-51[b]	H	c.6297_6298delAC	p.Pro2100Glyfs*54	Yes	Novel
KMS-52	H	c.4693 + 1G > T	splice site	Yes	Novel
KMS-53	H	c.10090C > T	p.Gln3364*	Yes	Novel
KMS-54	T	c.8401C > T	p.Arg2801*	Yes	Novel
KMS-56	H	c.15536G > A	p.Arg5179His	Yes	Ng et al. [2010]
KMS-58	H	c.4333T > G	p.Cys1445Gly	Yes	Novel
KMS-59	H	c.15256C > T	p.Arg5086*	Yes	Banka et al. [2012b]
KMS-60	H	c.11761C > T	p.Gln3921*	Unknown	Novel
KMS-61[c]	W	c.5269C > T	p.Arg1757*	Yes	Novel
KMS-62	H	c.15163_15168dup	p.Asp5055_Leu5056dup	Unknown[f]	Micale et al. [2011]
KMS-63	T	c.4577G > T	p.Cys1526Phe	Yes	Novel
KMS-69	H	c.11944C > T	p.Arg3982*	Yes	Paulussen et al. [2011]
KMS-70	T	c.13903C > T	p.Gln4635*	Yes	Novel
KMS-71[d]	T	c.12220C > T	p.Gln4074*	Unknown	Novel
KMS-72	T	c.15061C > T	p.Arg5021*	Yes	Banka et al. [2012b]
KMS-73	T	c.12274C > T	p.Gln4092*	Unknown	Micale et al. [2011]
KMS-76	T	c.4490_4491delAC	p.His1497Leufs*30	Yes	Novel
KMS-78	T	c.16338 + 1G > T	splice site	Yes	Novel
KMS-80	T	c.15088C > T	p.Arg5030Cys	Unknown	Makrythanasis et al. [2013]
KMS-82	T	c.3511G > T	p.Glu1171*	Yes	Novel
KMS-85	T	c.11722C > T	p.Gln3908*	Yes	Paulussen et al. [2011]
KMS-87	T	c.3281_3282delTC	p.Leu1094Profs*20	Yes	Novel
KMS-88	T	c.16052 + 1G > C	splice site	Unknown	Novel
KMS-91	T	c.4267C > T	p.Arg1423Cys	Unknown	Novel
Patients with *KDM6A* mutations					
KMS-31[e]	H	c.3717G > A	p.Trp1239*	Unknown	Miyake et al. [2013]
KMS-37[e]	H	c.1555C > T	p.Arg519*	Unknown	Miyake et al. [2013]
KMS-65[e]	H	c.3354_3356delTCT	p.Leu1119del	Yes	Miyake et al. [2013]
KMS-81	T	c.1909_1912delTCTA	p.Ser637Thrfs*53	Yes	Novel
KMS-83	T	c.4051C > T	p.Arg1351*	Unknown	Novel

H, high-resolution melting analysis/Sanger sequencing; T, targeted resequencing; W, whole exome sequencing.RefSeq NM_003482.3 for *MLL2* and RefSeq NM_021140.2 for *KDM6A* were used as reference sequences.

[a]References are listed when the same mutation has been reported previously.

[b]This patient was reported as proband 1 by Tekin et al. [2006].

[c]The detailed clinical features of this patient were reported by Ito et al. [2013] because of her hypothalamic pituitary complications.

[d]The clinical course of this patient, particularly the idiopathic thrombocytopenic purpura, was reported by Torii et al. [2009].

[e]These patients have been reported in our previous study [Miyake et al., 2013].

[f]Patient KMS-62: no mutation in the mother.

TABLE II. *MLL2* Non-Truncating-Type Mutations in Patients With KS

Amino acid change[a]	Patient ID	Domain	Polyphen-2 (score)	MutationTaster
p.Met1376Arg	KMS-22	—	Probably damaging (0.915)	Polymorphism
p.Arg1423Cys	KMS-91	PHD	Probably damaging (1.000)	Disease causing
p.Cys1445Gly	KMS-58	PHD	Probably damaging (1.000)	Disease causing
p.Cys1526Phe	KMS-63	PHD	Probably damaging (0.999)	Disease causing
p.Gln3277_Gln3282dup	KMS-02	—	NA	Polymorphism
p.Arg5030Cys	KMS-80	—	Probably damaging (1.000)	Disease causing
p.Asp5040Gly	KMS-15	—	Probably damaging (1.000)	Disease causing
p.Arg5048Cys	KMS-27	—	Probably damaging (1.000)	Disease causing
p.Arg5048His	KMS-38	—	Probably damaging (1.000)	Disease causing
p.Asp5055_Leu5056dup	KMS-40, 62	—	NA	Polymorphism
p.Arg5154Gln	KMS-23	—	Probably damaging (1.000)	Disease causing
p.Arg5179His	KMS-56	FYRN	Possibly damaging (0.840)	Disease causing
p.Gly5189Arg	KMS-49	FYRN	Probably damaging (1.000)	Disease causing
p.Arg5351Gln	KMS-42	—	Probably damaging (1.000)	Disease causing

[a]The nucleotide mutation nomenclature for these predicted protein mutations are included in Table I.

and $P = 0.1778$, respectively). Blue sclera, lower lip pits, spine/rib abnormality, hip joint dislocation, umbilical hernia, kidney dysfunction, cryptorchidism, liver abnormality, spleen abnormality, premature thelarche, neonatal hyperbilirubinemia, and anemia were observed only in the mutation-positive group.

Clinical Comparison of the *MLL2*-Mutated and *KDM6A*-Mutated Groups

We compared the clinical features between the *MLL2*-mutated and *KDM6A*-mutated groups (Figs. 3–5, Supplemental Table III). High arched eyebrows, short fifth fingers, and hypotonia in infancy were more frequent in individuals with *MLL2* mutations than in individuals with *KDM6A* mutations ($P = 0.0364$, 0.0039, and 0.0283, respectively). Short stature was more frequent in individuals with *KDM6A* mutations ($P = 0.0485$). Although not statistically significant, postnatal growth retardation was observed in all individuals with *KDM6A* mutations, whereas this was observed in only half of the individuals with *MLL2* mutations.

Clinical Comparison of Individuals With a *MLL2* Truncating-Type and Non-Truncating-Type Mutation

Most clinical features were observed at a similar ratio in both groups (Supplemental Table IV), except for prominent ears and hypotonia, which were more frequently observed in the truncating-type group than in the non-truncating-type group ($P = 0.0339$ and $P = 0.0248$, respectively). However, the facial appearance of individuals in the truncating-type group was more typical, based on the ten originally reported patients with KS [Kuroki et al., 1981; Niikawa et al., 1981], than that in the non-truncating-type group (Figs. 3 and 4). Except for patient KMS-58, the facial appearance of patients with a non-truncating-type mutation was rather less typical. It should be noted that these patients had thick eyebrows (not present in patient KMS-56). Furthermore, ectropion of the lower eyelid, depressed nasal tip, short columella, and prominent ears all seemed less obvious in the individuals with a non-truncating-type mutation.

X-Inactivation Pattern in Female Patients With a *KDM6A* Mutation

A *KDM6A* mutation was identified in two females (KMS-65 and KMS-81). Individual KMS-65 (c.3354_3356del, which predicts p.Leu1119del) showed a random X-inactivation pattern [Miyake et al., 2013], while individual KMS-81 with a frame-shift mutation showed marked skewing (98:2; Supplemental Fig. 1A). By RT-PCR using mRNA derived from a lymphoblastoid cell line from patient KMS-81, we confirmed that both the mutated and normal alleles were transcribed at similar levels when nonsense-mediated mRNA decay (NMD) was inhibited by cycloheximide treatment (Supplemental Fig. 1B). In untreated cells, or cells treated with dimethylsulfoxide (negative control), the mutant allele was transcribed at a lower level than the wild-type allele, indicating that NMD partially eliminated the mutant.

Exome Sequencing

Among the five patients who were also analyzed by whole exome sequencing, mutations were identified and later confirmed by Sanger sequencing in four (Table I). Fragments with an 11 base-pair insertion (c.3326_3336dup) of *MLL2* in patient KMS-21 could not be amplified by Ex Taq, but could be amplified by LA Taq with LA buffer and confirmed by Sanger sequencing. Three other mutations were missed by HRM analysis (Table I).

DISCUSSION

We identified 50 *MLL2* and five *KDM6A* mutations among 81 patients with KS and add to the 246 *MLL2* mutations described in patients with KS [Ng et al., 2010; Hannibal et al., 2011; Li et al., 2011; Micale et al., 2011; Paulussen et al., 2011; Banka et al., 2012a,b;

FIG. 3. Clinical features of patients with Kabuki syndrome harboring a MLL2 truncating-type mutation. A: Facial features of patients with Kabuki syndrome with a *MLL2* truncating-type mutation. The seven panels for patient KMS-54 show serial images at 0, 1, 4, 6.5, 9.5, 22, and 33 years of age, respectively. B: Complete right cleft lip/palate and lower lip pits (arrows) in patient KMS-41. C: Abnormal dentition in patients KMS-52 and KMS-59. They also showed hypodontia with wide interdentium. D: Patient KMS-72 had congenital strabismus and blepharoptosis as well as opacification of the cornea due to Peters anomaly (arrow). E: Hand images show short fifth fingers and prominent digit pads (white arrows).

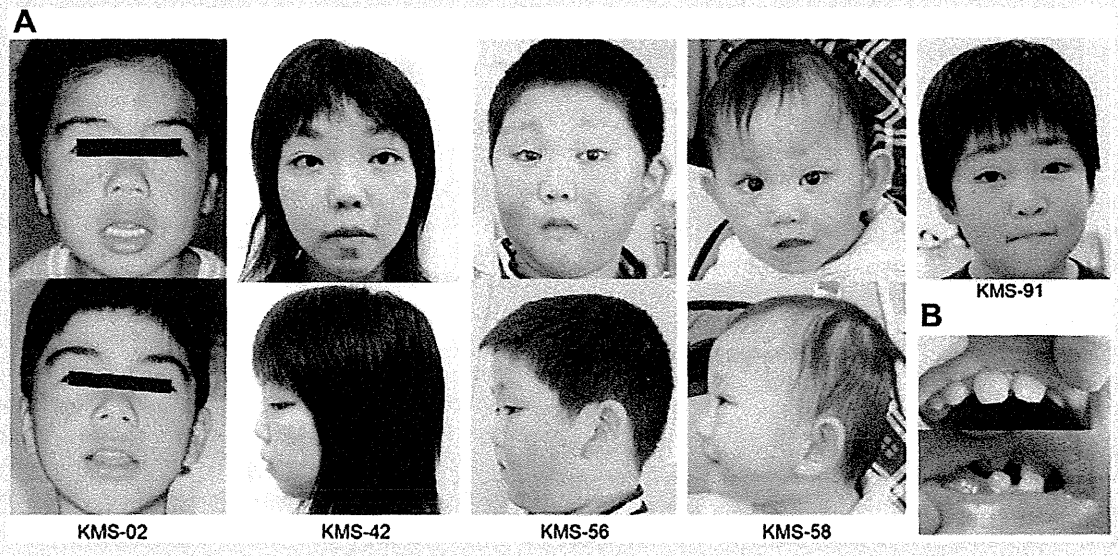

FIG. 4. Clinical features of patients with Kabuki syndrome with a *MLL2* non-truncating-type mutation. A: Facial features of patients with KS and a *MLL2* non-truncating-type mutation. B: Patient KMS-56 showed abnormal dentition [hypodontia with wide interdentium].

Kokitsu-Nakata et al., 2012; Tanaka et al., 2012; Bogershausen and Wollnik, 2013; Makrythanasis et al., 2013] (Human Gene Mutation Database Professional 2012.3; https://portal.biobase-international.com/hgmd/pro/gene.php). Our mutation-positivity rate for either gene was 67.9% (55/81), and that for *MLL2* only was 61.7% (50/81); these figures are compatible with those reported in a review (55–80%) [Banka et al., 2012b]. Mutation-negative patients suggest the existence of unknown genes to cause KS or misdiagnosis.

As for the phenotype–genotype relationship, Banka et al. [2012b] suggested that feeding problems, kidney anomalies, premature thelarche, joint dislocation, and palatal malformation were more frequently observed in patients with *MLL2*-mutations than in patients with normal *MLL2* sequence. Hannibal et al. [2011] reported that renal anomalies were more common in patients who had *MLL2* mutations compared to those who did not. Li et al. [2011] reported that short stature and renal anomalies were more frequent in patients with *MLL2*-mutations than in those with normal *MLL2* sequence. In our study, premature thelarche was observed only in patients with *MLL2* mutations, but this was not significant ($P = 0.1137$). The frequencies of kidney anomalies, hip joint dislocation, and short stature were not different when comparing those with and without *MLL2* mutations ($P = 0.3030$, $P = 1.0000$, and $P = 0.0717$, respectively; Supplemental Table V). High arched eyebrows, palatal malformation (cleft palate/lip), low posterior hairline, and short fifth finger were more frequently observed in individuals with *MLL2* mutations than in patients with normal *MLL2* ($P = 0.0118$, $P = 0.0284$, $P = 0.0493$, and $P = 0.0137$, respectively; Supplemental Table V).

X-inactivation skewing in patients with KS has been discussed since the discovery of the *KDM6A* deletion in a female with KS

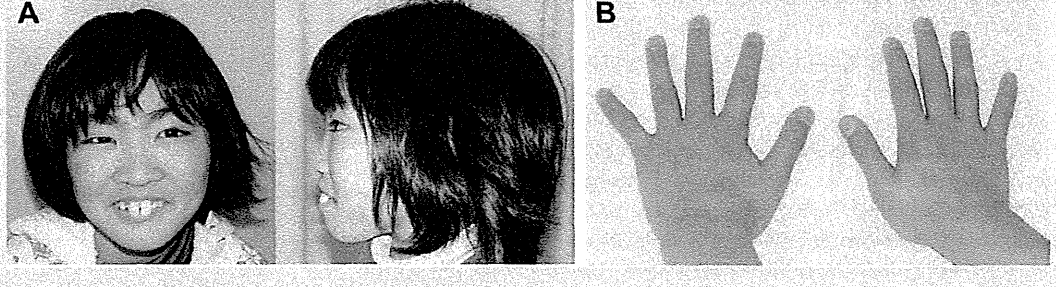

FIG. 5. Clinical features of patients with Kabuki syndrome with a *KDM6A* truncating-type mutation. A: Facial features of patient KMS-81 harboring a *KDM6A* mutation (c.1909_1912del, p.Ser637Thrfs*53). She showed large front teeth with wide interdentium. B: Hand image of KMS-81. Short fifth finger was not remarkable.

[Lederer et al., 2012; Miyake et al., 2013]. In two female patients reported here, patient KMS-65, who had an in-frame deletion, showed a random X-inactivation pattern, but patient KMS-81, who had a truncating-type mutation, showed marked skewing. X-inactivation skewing was also reported in two affected females with *KDM6A* deletion reported by Lederer et al. [2012]. cDNA sequence analysis of patient KMS-81 indicated that the mutant allele of *KDM6A* was expressed at a similar level to the wild-type allele under NMD inhibition. This result suggests that *KDM6A* mostly escapes X-inactivation in female lymphoblastoid cells. Interestingly, *KDM6A*/*Kdm6a* escapes X-inactivation in humans and mice, and in mice its expression level from the inactive X chromosome (Xi) was reported as 15–35% of that from the active X chromosome (Xa) [Greenfield et al., 1998; Xu et al., 2008]. We calculated the hypothetical expression assuming a 30% *KDM6A* expression level from Xi and 100% expression from Xa (Supplemental Fig. 2). In patient KMS-81, who showed marked skewing (98:2), either the mutant X chromosome or the wild-type X was inactivated in 98% of cells. If the mutant were inactivated, the expression level would be below 1 ($1.0 \times 0.98 + 0.3 \times 0.02 = 0.986$). If the wild-type were inactivated, the expression level would also be below 1 ($1.0 \times 0.02 + 0.3 \times 0.98 = 0.314$). The KS phenotype is usually unassociated with Turner syndrome (45,X), with the *KDM6A* expression level at 1.0 [Miyake et al., 2013]. It is possible that having a *KDM6A* expression level of 1.0 is essential for a normal human phenotype. Similarly, males with only one copy of *KDM6A* do not manifest KS. We previously mentioned the possibility of *UTY* compensation for *KMD6A* (Supplemental Fig. 2) [Miyake et al., 2013], although human UTY lacks demethylase activity [Hong et al., 2007; Lan et al., 2007]. The recent evidence that $X^{Utx-}X^{Utx-}$ homozygous mice demonstrated a more severe phenotype than $X^{Utx-}Y^{Uty+}$ mice indicates that UTY can compensate for the loss of UTX in embryonic development [Shpargel et al., 2012]. Because mouse and human UTY show 75% identity, and 95% identity in the Jumonji C domain [Shpargel et al., 2012], it is likely that normal human males who have only one copy of *KDM6A* are supplemented by *UTY* in a demethylase-independent manner.

Interestingly, $X^{Utx-}Y^{Uty+}$ mice showed small body size [Shpargel et al., 2012]. Similarly, the human *KDM6A*-mutated group exhibited short stature and postnatal growth retardation.

Regarding our mutation detection methods, HRM analysis and Sanger sequencing are both imperfect. Next-generation sequencing is more sensitive (especially for single nucleotide variants and small insertions/deletions), faster, and cheaper due to multiple gene screening and the potential to multiplex. However, a microdeletion involving *MLL2* or *KDM6A* or low-level mosaicism of a single nucleotide variant might be missed by this method. Therefore, in patients who test mutation-negative, more comprehensive approaches might be necessary. In conclusion, we investigated *MLL2* and *KDM6A* mutations and their clinical consequences in patients with KS. The majority of the clinical features were observed at a similar frequency among patients with either *MLL2* or *KDM6A*-mutations. The genetic basis of the patients who tested mutation-negative (20–45%) remains elusive. Further studies are necessary to understand the whole picture of the genetic aspects of KS and its genotype–phenotype relationships.

ACKNOWLEDGMENTS

We thank the patients and their parents for participating in this work. We also thank Ms. Y. Yamashita, Ms. E. Koike, Ms. S. Sugimoto, Ms. N. Watanabe, Ms. K. Takabe, and Mr. T. Miyama for their technical assistance. This work was supported by research grants from the Ministry of Health, Labour and Welfare of Japan (H. Saitsu, N. Matsumoto, N. Miyake), the Japan Science and Technology Agency (N. Matsumoto), the Strategic Research Program for Brain Sciences (N. Matsumoto), a Grant-in-Aid for Scientific Research on Innovative Areas-(Transcription cycle)-from the Ministry of Education, Culture, Sports, Science and Technology of Japan (N. Matsumoto), a Grant-in-Aid for Scientific Research from the Japan Society for the Promotion of Science (N. Matsumoto), a Grant-in-Aid for Young Scientists from the Japan Society for the Promotion of Science (H.S., N. Miyake), the Takeda Science Foundation (N. Matsumoto, N. Miyake), the Yokohama Foundation for the Advancement of Medical Science (N. Miyake), and the Hayashi Memorial Foundation for Female Natural Scientists (N. Miyake).

REFERENCES

Adzhubei IA, Schmidt S, Peshkin L, Ramensky VE, Gerasimova A, Bork P, Kondrashov AS, Sunyaev SR. 2010. A method and server for predicting damaging missense mutations. Nat Methods 7:248–249.

Allen RC, Zoghbi HY, Moseley AB, Rosenblatt HM, Belmont JW. 1992. Methylation of *Hpa*II and *Hha*I sites near the polymorphic CAG repeat in the human androgen-receptor gene correlates with X chromosome inactivation. Am J Hum Genet 51:1229–1239.

Banka S, Howard E, Bunstone S, Chandler K, Kerr B, Lachlan K, McKee S, Mehta S, Tavares A, Tolmie J, Donnai D. 2012a. MLL2 mosaic mutations and intragenic deletion-duplications in patients with Kabuki syndrome. Clin Genet 83:467–471.

Banka S, Veeramachaneni R, Reardon W, Howard E, Bunstone S, Ragge N, Parker MJ, Crow YJ, Kerr B, Kingston H, Metcalfe K, Chandler K, Magee A, Stewart F, McConnell VP, Donnelly DE, Berland S, Houge G, Morton JE, Oley C, Revencu N, Park SM, Davies SJ, Fry AE, Lynch SA, Gill H, Schweiger S, Lam WW, Tolmie J, Mohammed SN, Hobson E, Smith A, Blyth M, Bennett C, Vasudevan PC, Garcia-Minaur S, Henderson A, Goodship J, Wright MJ, Fisher R, Gibbons R, Price SM, CdS D, Temple IK, Collins AL, Lachlan K, Elmslie F, McEntagart M, Castle B, Clayton-Smith J, Black GC, Donnai D. 2012b. How genetically heterogeneous is Kabuki syndrome?: MLL2 testing in 116 patients, review and analyses of mutation and phenotypic spectrum. Eur J Hum Genet 20:381–388.

Bogershausen N, Wollnik B. 2013. Unmasking Kabuki syndrome. Clin Genet 83:201–211.

Dubuc AM, Remke M, Korshunov A, Northcott PA, Zhan SH, Mendez-Lago M, Kool M, Jones DT, Unterberger A, Morrissy AS, Shih D, Peacock J, Ramaswamy V, Rolider A, Wang X, Witt H, Hielscher T, Hawkins C, Vibhakar R, Croul S, Rutka JT, Weiss WA, Jones SJ, Eberhart CG, Marra MA, Pfister SM, Taylor MD. 2013. Aberrant patterns of H3K4 and H3K27 histone lysine methylation occur across subgroups in medulloblastoma. Acta Neuropathol 125:373–384.

Greenfield A, Carrel L, Pennisi D, Philippe C, Quaderi N, Siggers P, Steiner K, Tam PP, Monaco AP, Willard HF, Koopman P. 1998. The UTX gene escapes X inactivation in mice and humans. Hum Mol Genet 7:737–742.

Hannibal MC, Buckingham KJ, Ng SB, Ming JE, Beck AE, McMillin MJ, Gildersleeve HI, Bigham AW, Tabor HK, Mefford HC, Cook J, Yoshiura K, Matsumoto T, Matsumoto N, Miyake N, Tonoki H, Naritomi K,

Kaname T, Nagai T, Ohashi H, Kurosawa K, Hou JW, Ohta T, Liang D, Sudo A, Morris CA, Banka S, Black GC, Clayton-Smith J, Nickerson DA, Zackai EH, Shaikh TH, Donnai D, Niikawa N, Shendure J, Bamshad MJ. 2011. Spectrum of MLL2 (ALR) mutations in 110 cases of Kabuki syndrome. Am J Med Genet Part A 155A:1511–1516.

Hong S, Cho YW, Yu LR, Yu H, Veenstra TD, Ge K. 2007. Identification of JmjC domain-containing UTX and JMJD3 as histone H3 lysine 27 demethylases. Proc Natl Acad Sci USA 104:18439–18444.

Ito N, Ihara K, Tsutsumi Y, Miyake N, Matsumoto N, Hara T. 2013. Hypothalamic pituitary complications in Kabuki syndrome. Pituitary 16:133–138.

Kokitsu-Nakata NM, Petrin AL, Heard JP, Vendramini-Pittoli S, Henkle LE, dos Santos DV, Murray JC, Richieri-Costa A. 2012. Analysis of MLL2 gene in the first Brazilian family with Kabuki syndrome. Am J Med Genet Part A 158A:2003–2008.

Kuroki Y, Suzuki Y, Chyo H, Hata A, Matsui I. 1981. A new malformation syndrome of long palpebral fissures, large ears, depressed nasal tip, and skeletal anomalies associated with postnatal dwarfism and mental retardation. J Pediatr 99:570–573.

Lan F, Bayliss PE, Rinn JL, Whetstine JR, Wang JK, Chen S, Iwase S, Alpatov R, Issaeva I, Canaani E, Roberts TM, Chang HY, Shi Y. 2007. A histone H3 lysine 27 demethylase regulates animal posterior development. Nature 449:689–694.

Lederer D, Grisart B, Digilio MC, Benoit V, Crespin M, Ghariani SC, Maystadt I, Dallapiccola B, Verellen-Dumoulin C. 2012. Deletion of KDM6A, a histone demethylase interacting with MLL2, in three patients with Kabuki syndrome. Am J Hum Genet 90:119–124.

Lee MG, Villa R, Trojer P, Norman J, Yan KP, Reinberg D, Di Croce L, Shiekhattar R. 2007. Demethylation of H3K27 regulates polycomb recruitment and H2A ubiquitination. Science 318:447–450.

Li Y, Bogershausen N, Alanay Y, Simsek Kiper PO, Plume N, Keupp K, Pohl E, Pawlik B, Rachwalski M, Milz E, Thoenes M, Albrecht B, Prott EC, Lehmkuhler M, Demuth S, Utine GE, Boduroglu K, Frankenbusch K, Borck G, Gillessen-Kaesbach G, Yigit G, Wieczorek D, Wollnik B. 2011. A mutation screen in patients with Kabuki syndrome. Hum Genet 130:715–724.

Makrythanasis P, van Bon BW, Steehouwer M, Rodriguez-Santiago B, Simpson M, Dias P, Anderlid BM, Arts P, Bhat M, Augello B, Biamino E, Bongers EM, Del Campo M, Cordeiro I, Cueto-Gonzalez AM, Cusco I, Deshpande C, Frysira E, Louise I, Flores R, Galan E, Gener B, Gilissen C, Granneman SM, Hoyer J, Yntema HG, Kets CM, Koolen DA, Marcelis CL, Medeira A, Micale L, Mohammed S, de Munnik SA, Nordgren A, Reardon SP, Revencu N, Roscioli T, Ruiterkamp-Versteeg M, Santos HG, Schoumans J, Schuurs-Hoeijmakers JH, Silengo MC, Toledo L, Vendrell T, van der Burgt I, van Lier B, Zweier C, Reymond A, Trembath RC, Perez-Jurado L, Dupont J, de Vries BB, Brunner HG, Veltman JA, Merla G, Antonarakis SE, Hoischen A. 2013. MLL2 mutation detection in 86 patients with Kabuki syndrome: A genotype–phenotype study. Clin Genet (In Press).

Micale L, Augello B, Fusco C, Selicorni A, Loviglio MN, Silengo MC, Reymond A, Gumiero B, Zucchetti F, D'Addetta EV, Belligni E, Calcagni A, Digilio MC, Dallapiccola B, Faravelli F, Forzano F, Accadia M, Bonfante A, Clementi M, Daolio C, Douzgou S, Ferrari P, Fischetto R, Garavelli L, Lapi E, Mattina T, Melis D, Patricelli MG, Priolo M, Prontera P, Renieri A, Mencarelli MA, Scarano G, della Monica M, Toschi B, Turolla L, Vancini L, Zatterale A, Gabrielli O, Zelante L, Merla G. 2011. Mutation spectrum of MLL2 in a cohort of Kabuki syndrome patients. Orphanet J Rare Dis 6:38.

Miyake N, Mizuno S, Okamoto N, Ohashi H, Shiina M, Ogata K, Tsurusaki Y, Nakashima M, Saitsu H, Niikawa N, Matsumoto N. 2013. KDM6A point mutations cause Kabuki syndrome. Hum Mutat 34:108–110.

Ng SB, Bigham AW, Buckingham KJ, Hannibal MC, McMillin MJ, Gildersleeve HI, Beck AE, Tabor HK, Cooper GM, Mefford HC, Lee C, Turner EH, Smith JD, Rieder MJ, Yoshiura K, Matsumoto N, Ohta T, Niikawa N, Nickerson DA, Bamshad MJ, Shendure J. 2010. Exome sequencing identifies MLL2 mutations as a cause of Kabuki syndrome. Nat Genet 42:790–793.

Niikawa N, Matsuura N, Fukushima Y, Ohsawa T, Kajii T. 1981. Kabuki make-up syndrome: A syndrome of mental retardation, unusual facies, large and protruding ears, and postnatal growth deficiency. J Pediatr 99:565–569.

Niikawa N, Kuroki Y, Kajii T, Matsuura N, Ishikiriyama S, Tonoki H, Ishikawa N, Yamada Y, Fujita M, Umemoto H, Iwama Y, Kondoh I, Fukushima Y, Nako Y, Matsui I, Urakami T, Aritaki S, Hara M, Suzuki Y, Chyo H, Sugio Y, Hasegawa T, Yamanaka T, Tsukino R, Yoshida A, Nomoto N, Kawahito S, Aihara R, Toyota S, Ieshima A, Funaki H, Ishitobi K, Ogura S, Furumae T, Yoshino M, Tsuji Y, Kondoh T, Matsumoto T, Abe K, Harada N, Miike T, Ohdo S, Naritomi K, Abushwereb AK, Braun OH, Schmid E. 1988. Kabuki make-up (Niikawa–Kuroki) syndrome: A study of 62 patients. Am J Med Genet 31:565–589.

Paulussen AD, Stegmann AP, Blok MJ, Tserpelis D, Posma-Velter C, Detisch Y, Smeets EE, Wagemans A, Schrander JJ, van den Boogaard MJ, van der Smagt J, van Haeringen A, Stolte-Dijkstra I, Kerstjens-Frederikse WS, Mancini GM, Wessels MW, Hennekam RC, Vreeburg M, Geraedts J, de Ravel T, Fryns JP, Smeets HJ, Devriendt K, Schrander-Stumpel CT. 2011. MLL2 mutation spectrum in 45 patients with Kabuki syndrome. Hum Mutat 32:E2018–E2025.

Prasad R, Zhadanov AB, Sedkov Y, Bullrich F, Druck T, Rallapalli R, Yano T, Alder H, Croce CM, Huebner K, Mazo A, Canaani E. 1997. Structure and expression pattern of human ALR, a novel gene with strong homology to ALL-1 involved in acute leukemia and to Drosophila trithorax. Oncogene 15:549–560.

Schuettengruber B, Chourrout D, Vervoort M, Leblanc B, Cavalli G. 2007. Genome regulation by polycomb and trithorax proteins. Cell 128:735–745.

Schwarz JM, Rodelsperger C, Schuelke M, Seelow D. 2010. MutationTaster evaluates disease-causing potential of sequence alterations. Nat Methods 7:575–576.

Shpargel KB, Sengoku T, Yokoyama S, Magnuson T. 2012. UTX and UTY demonstrate histone demethylase-independent function in mouse embryonic development. PLoS Genet 8:e1002964.

Tanaka R, Takenouchi T, Uchida K, Sato T, Fukushima H, Yoshihashi H, Takahashi T, Tsubota K, Kosaki K. 2012. Congenital corneal staphyloma as a complication of Kabuki syndrome. Am J Med Genet Part A 158A:2000–2002.

Tekin M, Fitoz S, Arici S, Cetinkaya E, Incesulu A. 2006. Niikawa–Kuroki (Kabuki) syndrome with congenital sensorineural deafness: Evidence for a wide spectrum of inner ear abnormalities. Int J Pediatr Otorhinolaryngol 70:885–889.

Torii Y, Yagasaki H, Tanaka H, Mizuno S, Nishio N, Muramatsu H, Hama A, Takahashi Y, Kojima S. 2009. Successful treatment with rituximab of refractory idiopathic thrombocytopenic purpura in a patient with Kabuki syndrome. Int J Hematol 90:174–176.

Tsurusaki Y, Kobayashi Y, Hisano M, Ito S, Doi H, Nakashima M, Saitsu H, Matsumoto N, Miyake N. 2013. The diagnostic utility of exome sequencing in Joubert syndrome and related disorders. J Hum Genet 58:113–115.

Xu J, Deng X, Watkins R, Disteche CM. 2008. Sex-specific differences in expression of histone demethylases Utx and Uty in mouse brain and neurons. J Neurosci 28:4521–4527.

INTERNAL MEDICINE

CASE REPORT

Identification of a Novel Homozygous *SPG7* Mutation in a Japanese Patient with Spastic Ataxia: Making an Efficient Diagnosis Using Exome Sequencing for Autosomal Recessive Cerebellar Ataxia and Spastic Paraplegia

Hiroshi Doi[1,2], Chihiro Ohba[1,2], Yoshinori Tsurusaki[1], Satoko Miyatake[1], Noriko Miyake[1], Hirotomo Saitsu[1], Yuko Kawamoto[2], Tamaki Yoshida[2], Shigeru Koyano[2], Yume Suzuki[2], Yoshiyuki Kuroiwa[2], Fumiaki Tanaka[2] and Naomichi Matsumoto[1]

Abstract

Autosomal recessive cerebellar ataxias and autosomal recessive hereditary spastic paraplegias are clinically and genetically heterogeneous disorders with diverse neurological and non-neurological features. We herein describe a Japanese patient with a slowly progressive form of ataxia and spastic paraplegia. Using whole exome sequencing, we identified a novel homozygous frameshift mutation in *SPG7*, encoding paraplegin, in this patient. This is the first report of an *SPG7* mutation in the Japanese population. For disorders previously undetected in a particular population, or unrecognized/atypical phenotypes, exome sequencing may facilitate molecular diagnosis.

Key words: cerebellar ataxia, spastic paraplegia, exome, *SPG7*, paraplegin

(Intern Med 52: 1629-1633, 2013)
(DOI: 10.2169/internalmedicine.52.0252)

Introduction

Hereditary ataxias and hereditary spastic paraplegias (HSPs) are clinically and genetically heterogeneous neurological disorders exhibiting an autosomal dominant, autosomal recessive or X-linked mode of inheritance. Mutations in more than 30 different genes have been identified for autosomal recessive cerebellar ataxias (ARCAs) (1-3), and mutations in over 22 different genes have been identified for autosomal recessive hereditary spastic paraplegias (ARHSPs) (4-6). Both disorders are generally associated with diverse neurological and non-neurological symptoms that partially overlap, resulting in complex phenotypes. Furthermore, while these disorders can be caused by mutations in the same gene, the phenotypes can vary. Therefore, genetic diagnostic tests for ARCAs and ARHSPs are complex and time-consuming. In this study, we describe a Japanese patient exhibiting a slowly progressive form of spastic ataxia. Using whole exome sequencing, we identified a causative mutation in *SPG7* that has not been previously detected in the Japanese population.

Case Report

Clinical information and a blood sample were obtained from the patient after he provided his written informed consent. The experimental protocols were approved by the Institutional Review Board of Yokohama City University School of Medicine. Among the children of first-cousin parents, two were affected (including the proband), while two were healthy (Figure A). DNA was available from the proband only, who is now 64 years old. Arrhythmic episodes commenced at 6 years of age. At 34 years of age, he experienced stiffness in the legs after protracted periods in the cold and stumbled when moving swiftly. At -40 years of

[1]Department of Human Genetics, Yokohama City University, Japan and [2]Department of Clinical Neurology and Stroke Medicine, Yokohama City University, Japan
Received for publication January 29, 2013; Accepted for publication March 25, 2013
Correspondence to Dr. Naomichi Matsumoto, naomat@yokohama-cu.ac.jp

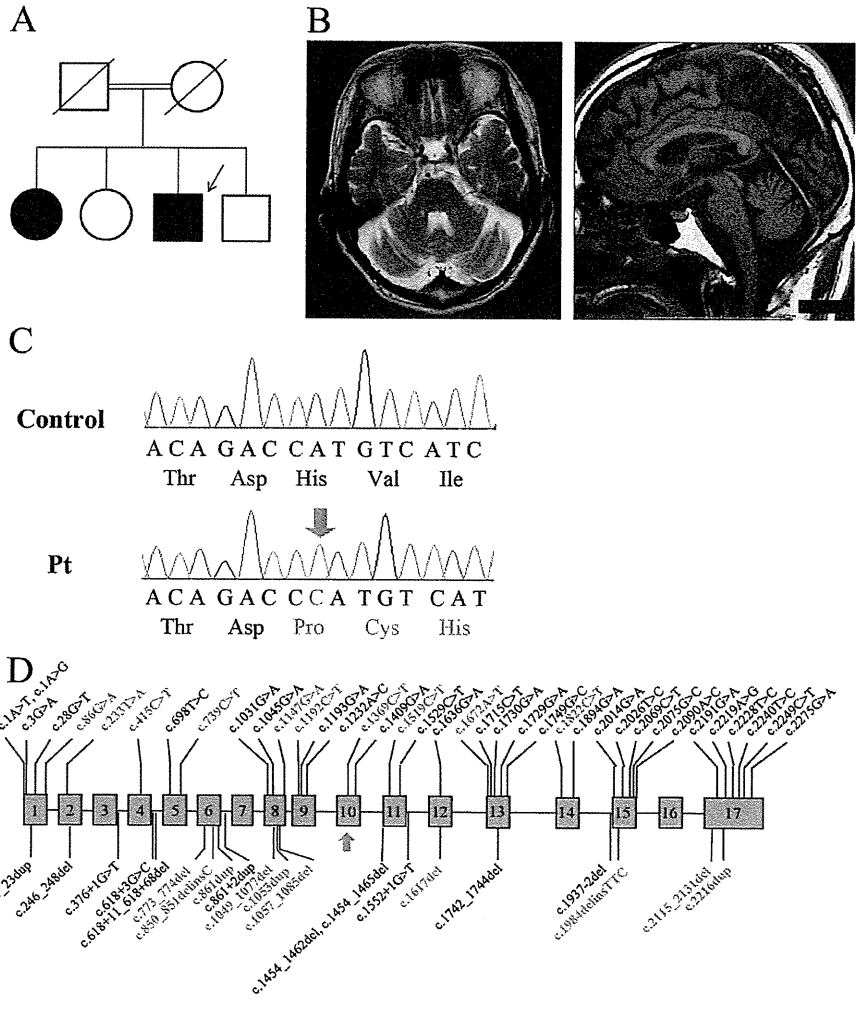

Figure. **Phenotypic and genotypic analyses of the patient. (a) Family pedigree. The arrow indicates the proband. (b) Brain magnetic resonance imaging of the patient at 62 years of age. Axial section of a T2-weighted image (left panel) and sagittal section of a T1-weighted image (right panel). Moderate atrophy of the cerebellar hemispheres was revealed. The corpus callosum was normal. (c) Electropherograms of a control with the *SPG7* wild-type sequence (upper) and the patient with a homozygous mutation (lower). The single-base insertion c.1342dup is indicated by a red arrow. (d) Known *SPG7* mutations (7, 8, 11-15, 20-22). The mutations predicted to generate a premature stop codon are indicated by red letters; c.1342dup is indicated by a red arrow.**

age, he felt stiffness in the legs after walking 5 kilometers and had difficulty moving briskly. At 47 years of age, he was examined in the hospital where he was diagnosed with a complicated form of HSP. At 49 years of age, he displayed slurred speech. These symptoms gradually worsened, and, at 54 years of age, he started using a cane when walking. He was admitted to our hospital for a clinical evaluation. He exhibited a disturbance of smooth pursuit eye movements as well as mild omnidirectional gaze palsy, dysarthria, pronounced spasticity and mild weakness of the lower extremities, extensor plantar reflexes (Babinski sign) and truncal instability. While the patellar tendon reflexes and Achilles tendon reflexes were increased, no knee or ankle clonus were observed. No pes cavus, muscle atrophy, fasciculation, involuntary movements, autonomic involvement or sensory involvement were observed. The patient exhibited slight cognitive decline. His score on a revised version of the Hasegawa Dementia Scale (HDS) was 24/30. The frontal assessment battery score was 13/18, indicating slight frontal lobe dysfunction. Laboratory biochemistry results were normal, including the levels of serum albumin, vitamin E and very long chain fatty acids. A nerve conduction study disclosed no neuropathy, and an ophthalmic evaluation revealed no ocular atrophy. Brain magnetic resonance imaging revealed moderate atrophy of the cerebellar hemispheres; however, no hypoplasia/atrophy of the corpus callosum, brain stem or cerebral cortex was observed (Figure B). The patient was diagnosed with ARCA, taking into consideration the

dysarthria and cerebellar atrophy.

The patient was 64 years old at the last examination. He displayed moderate omnidirectional gaze palsy, impaired vertical and horizontal optokinetic nystagmus and slow saccade. Mild limb ataxia was also observed. Muscle weakness of the lower extremities was advanced, especially in the hamstrings and anterior tibial muscles (manual muscle testing 2-3), consistent with disturbance of the pyramidal tracts. He was unable to walk without holding on to something due to spasticity and muscle weakness. His cognitive impairment did not progress (HDS 22/30, Mini-Mental State Examination 26/30).

Exome sequencing

To identify the causative mutation, whole exome sequencing was performed on the patient's DNA. Genomic DNA was processed using a SureSelect Human All Exon Kit (50 Mb; Agilent Technologies, Santa Clara, CA) according to the manufacturer's instructions. Captured DNAs were sequenced using a GAIIx sequencer (Illumina, San Diego, CA). Approximately 44.9 million paired-reads were mapped to the human reference genome. A coverage analysis revealed that 88.9% of the bases within the target regions were covered by 10 reads or more. We checked whether mutations were present in known ARCA or ARHSP genes. For 36/59 of the relevant genes, more than 90% of the entire coding sequence was covered by 10 reads or more (Table). A homozygous frameshift mutation, c.1342dup (NM_003119.2; p.His448Profs*12), was identified in exon 10 of *SPG7* (16q24.3, MIM 602783). Sanger sequencing on an ABI 3500xL (Life Technologies, Carlsbad, CA) confirmed c.1342dup homozygosity in the patient (Figure C). No mutations were detected using Sanger sequencing in the other exons of *SPG7*. The mutation was undetected in 752 control alleles. No other mutations located in exons or splice sites were detected among the 59 relevant genes.

Discussion

In this report, we described a case of an adult-onset slowly progressive form of spastic ataxia. Using whole exome sequencing, we were able to identify a novel homozygous frameshift mutation, c. 1342 dup (p.His448Profs*12) in *SPG7*. *SPG7* was the first gene identified in ARHSP (7). Mutations in *SPG7* are known to cause both pure and complicated HSP phenotypes. In complicated forms, the clinical symptoms can be accompanied by cerebellar syndrome, optic neuropathy, supranuclear palsy and cognitive impairments (8-10). Although mutations in *SPG7* account for just under 5% of ARHSP cases in Europe (11), they have never been found in a Japanese population.

SPG7 encodes paraplegin, a nuclear DNA-encoded mitochondrial metalloprotease belonging to the adenosine triphosphatases associated with diverse cellular activities (AAA) family of proteins. Loss of the function of paraplegin leads to mitochondrial dysfunction. The p.His448Profs*12 mutation is predicted to result in a premature stop codon. Previous reports (7, 9-15) have revealed that missense and nonsense mutations located closer to the C-terminal of paraplegin than the p.His448Profs*12 mutation can cause disease (Figure D). Recently, genotype-phenotype correlations were identified for *SPG7*: an association between cerebellar ataxia and *SPG7* null alleles leading to an absence of protein products or severely truncated protein products and an association between optic nerve atrophy and a missense mutation in exon 10 (pArg470Gln) (9). The clinical phenotype observed in our patient, who had cerebellar ataxia without optic nerve atrophy, is compatible with an *SPG7* mutation. We concluded that the homozygous p.His448Profs*12 mutation was deleterious and causative of the patient's clinical phenotype.

Because there are regional differences in the prevalence of recessive disorders, it is difficult to perform genetic testing for rare and heterogeneous disorders, especially when they have not been previously reported in the population. The relative frequencies of ARCAs and HSPs in patients with spinocerebellar ataxia spectrum disorders (including sporadic and hereditary cases) are estimated to be 1.8% and 4.7%, respectively (16). Although the precise prevalence of each subtype of ARCA and ARHSP remains unknown, the relatively common ARCAs and ARHSPs observed in Japan are ataxia, early-onset, with oculomotor apraxia and hypoalbuminemia/ataxia-oculomotor apraxia 1 (MIM 208920), ataxia-oculomotor apraxia 2 (MIM 606002), ataxia with isolated vitamin E deficiency (MIM 277460), ataxia-telangiectasia (MIM 208900), spastic ataxia, Charlevoix-Saguenay type (MIM 270550) and spastic paraplegia 11 (MIM 604360) (17). The clinical phenotype of our patient was not fully consistent with ARCA/ARHSPs previously reported in Japan. Considering the clinical and genetic diversity among ARCA/ARHSPs, we selected whole exome sequencing as the diagnostic method. Friedreich ataxia 1 (MIM 229300), which is primarily caused by the expansion of a trinucleotide repeat in *FXN*, may be undetectable by exome sequencing. However, an *FXN* mutation has never been described in the Japanese population, even though the gene has been tested for in suspected cases. In these cases, whole exome sequencing is the most promising method for identifying a causative mutation in one of the known ARCA or ARHSP genes. Indeed, most ARCA and ARHSP genes were covered by our exome sequencing approach, with the exception of the few genes that had low read-coverage, such as *KIAA0415* and *GJC2* (Table). More recently, the read-coverage was improved by upgrading the bait design (Table).

Recently, it became feasible to use whole exome sequencing for diagnostic purposes. Even for disorders previously undetected in a particular population, or unrecognized/atypical phenotypes, exome sequencing may facilitate molecular diagnosis (18, 19). In our case, the diagnosis varied, depending on whether the clinicians emphasized pyramidal or cerebellar signs. We believe that a diagnosis provided by

Table. **Read Coverage of ARCA and ARHSP Genes**

Disease	Gene	Covered by 10 or more reads	
		50Mb	51Mb
Friedrich ataxia	*FXN*	70.5	76.2
Ataxia with isolated vitamin E deficiency	*TTPA (TTP1)*	75.7	78.6
Ataxia, early-onset, with oculomotor apraxia and hypoalbuminemia	***APTX***	**100**	**95.1**
Abetalipoproteinemia	***MTTP***	**100**	**98.8**
Refsum disease	***PHYH***	**92.6**	**98.4**
	PEX7	86.7	87.7
Late-onset Tay-Sachs disease	***HEXA***	**100**	**96**
Cerebrotendinous xanthomatosis	*CYP27A1*	88.5	**97.9**
DNA polymerase g disorders	*POLG*	89.1	**97.4**
Ataxia talangiectasia	***ATM***	**100**	**100**
Ataxia talangiectasia-like disorder	***MRE11B (MRE11A)***	**100**	**98.8**
Autosomal recessive ataxia of Charlevoix-Saguenay	***SACS***	**98.9**	**99.4**
Mitochondrial DNA depletion syndrome 7	***C10orf2 (PEO1)***	**100**	**98.7**
Cayman ataxia	*ATCAY*	87.1	**97.4**
Marinesco-Sjogren syndrome	*SIL1*	76.1	**98.3**
SCAR1 (Ataxia-oculomotor apraxia 2)	***SETX***	**100**	**100**
SCAR5	***ZNF592***	**97.5**	**92.5**
SCAR8	***SYNE1***	**100**	**98.8**
SCAR9	*ADCK3 (CABC1)*	84.2	**97.9**
SCAR10	***ANO10 (TREM16K)***	**92.4**	**99.6**
SCAR11	***SYT14***	**92**	**91.8**
SCAN1	***TDP1***	**100**	**95.6**
SPAX3	***MARS2***	**96.0**	**100**
SPAX4	***MTPAP***	**100**	**91.0**
SPAX5	***AFG3L2***	**95.2**	**95.2**
Ataxia & Encephalopathy	*TTC19*	88.1	71.1
Ataxia with oculomotor apraxia 3 (AOA3)	*PIK3R5*	67.8	**97.4**
Dilated cardiomyopathy with ataxia	***DNAJC19 (TIM14)***	**98.9**	78.7
Epilepsy, progressive myoclonic 6	***GOSR2***	**96.3**	**99.7**
Karak syndrome	*PLA2G6*	73.1	**97**
Myoclonus epilepsy of Unverricht-Lundborg	*CSTB*	77.7	78.4
Action myoclonus renal failure / Progressive myoclonus epilepsy without renal failure	***SCARB2***	**95.2**	**100**
Progressive myoclonus epilepsy-ataxia syndrome	***PRICKLE1***	**100**	**99.7**
Refsum-like disorder	***ABHD12***	**90.5**	**94.1**
Posterior column ataxia & Retinitis pigmentosa	*FLVCR1*	80.3	89.5
Seizures, sensorineural deafness, ataxia, mental retardation, electrolyte imbalance (SeSAME)	***KCNJ10***	**100**	**100**
α-Methylacyl-CoA racemase (AMACR) deficiency	*AMACR*	80.1	**98.5**
Niemann-Pick, Type C	***NPC1***	**98.3**	**96.1**
	NPC2	77.2	**100**
Wilson disease	***ATP7B***	**95.6**	**95.9**
SPG5A	***CYP7B1***	**91.9**	**94.9**
SPG7	***SPG7***	**92**	89.9
SPG11	***KIAA1840 (SPG11)***	**96.1**	**99.3**
SPG15	***SPG15 (ZFYVE26)***	**99**	**92**
SPG18	***ERLIN2***	**100**	84.3
SPG20	***SPG20***	**100**	**100**
SPG21	***SPG21***	**100**	**99.7**
SPG28	*DDHD1*	84.4	**93**
SPG30	*KIF1A*	74.4	**92.5**
SPG35	*FA2H*	58.6	70.2
SPG39	*PNPLA6*	61.7	**97.5**
SPG44	*GJC2*	29.2	71.6
SPG46	***GBA2***	**100**	**100**
SPG47	***AP4B1***	**100**	**100**
SPG48	*KIAA0415*	51	88
SPG49	***TECPR2***	**92.4**	**99.5**
SPG50	***AP4M1***	**90.6**	**98.7**
SPG51	***AP4E1***	**95.6**	**96.6**
SPG52	*AP4S1*	87.9	**92**
SPG53	*VPS37A*	89.5	**96**
SPG54	***DDHD2***	**100**	**99.5**
SPG55	***C12orf65***	**100**	**97.1**
SPG56	*CYP2U1*	70.1	**91.9**

The percentage of coding sequence covered by 10 or more reads. The 50Mb column shows data for our patient; the 51 Mb column shows reference data from 4 patients with other diseases and whose DNA was processed using the latest version of SureSelect Human All Exon Kit. Genes with > 90% of the total coding sequence covered by 10 or more reads are highlighted in bold.

exome sequencing would improve the quality of clinical evaluation in patients with rare diseases.

The authors state that they have no Conflict of Interest (COI).

Acknowledgement

We would like to thank the patient and his family for their participation in this study.

Funding

This work was supported by Research Grants from the Ministry of Health, Labour and Welfare (N. Miyake, H.S., F.T. and N. Matsumoto) and the Japan Science and Technology Agency (N. Matsumoto), the Strategic Research Program for Brain Sciences (N. Matsumoto) and a Grant-in-Aid for Scientific Research on Innovative Areas from the Ministry of Education, Culture, Sports, Science and Technology of Japan (F.T. and N. Matsumoto), a Grant-in-Aid for Scientific Research from the Japan Society for the Promotion of Science (S.K., F.T., Y. Kuroiwa and N. Matsumoto), a Grant-in-Aid for Young Scientists from the Japan Society for the Promotion of Science (H.D., N. Miyake and H.S.), a grant from the 2011 Strategic Research Promotion of Yokohama City University (N. Matsumoto), Research Grants from the Japan Epilepsy Research Foundation (H.S.) and the Takeda Science Foundation (N. Matsumoto and N. Miyake).

References

1. Palau F, Espinos C. Autosomal recessive cerebellar ataxias. Orphanet J Rare Dis **1**: 47, 2006.
2. Manto M, Marmolino D. Cerebellar ataxias. Curr Opin Neurol **22**: 419-429, 2009.
3. Vermeer S, Hoischen A, Meijer RP, et al. Targeted next-generation sequencing of a 12.5 Mb homozygous region reveals *ANO10* mutations in patients with autosomal-recessive cerebellar ataxia. Am J Hum Genet **87**: 813-819, 2010.
4. Blackstone C, O'Kane CJ, Reid E. Hereditary spastic paraplegias: membrane traffic and the motor pathway. Nat Rev Neurosci **12**: 31-42, 2011.
5. Erlich Y, Edvardson S, Hodges E, et al. Exome sequencing and disease-network analysis of a single family implicate a mutation in *KIF1A* in hereditary spastic paraparesis. Genome Res **21**: 658-664, 2011.
6. Alazami AM, Adly N, Al Dhalaan H, Alkuraya FS. A nullimorphic *ERLIN2* mutation defines a complicated Hereditary Spastic Paraplegia locus (SPG18). Neurogenetics **12**: 333-336, 2011.
7. Casari G, De Fusco M, Ciarmatori S, et al. Spastic paraplegia and OXPHOS impairment caused by mutations in paraplegin, a nuclear-encoded mitochondrial metalloprotease. Cell **93**: 973-983, 1998.
8. Warnecke T, Duning T, Schwan A, Lohmann H, Epplen JT, Young P. A novel form of autosomal recessive hereditary spastic paraplegia caused by a new *SPG7* mutation. Neurology **69**: 368-375, 2007.
9. van Gassen KL, van der Heijden CD, de Bot ST, et al. Genotype-phenotype correlations in spastic paraplegia type 7: a study in a large Dutch cohort. Brain **135**: 2994-3004, 2012.
10. Klebe S, Depienne C, Gerber S, et al. Spastic paraplegia gene 7 in patients with spasticity and/or optic neuropathy. Brain **135**: 2980-2993, 2012.
11. Elleuch N, Depienne C, Benomar A, et al. Mutation analysis of the paraplegin gene (*SPG7*) in patients with hereditary spastic paraplegia. Neurology **66**: 654-659, 2006.
12. Schlipf NA, Schule R, Klimpe S, et al. Amplicon-based high-throughput pooled sequencing identifies mutations in *CYP7B1* and *SPG7* in sporadic spastic paraplegia patients. Clin Genet **80**: 148-160, 2011.
13. Arnoldi A, Tonelli A, Crippa F, et al. A clinical, genetic, and biochemical characterization of *SPG7* mutations in a large cohort of patients with hereditary spastic paraplegia. Hum Mutat **29**: 522-531, 2008.
14. Tzoulis C, Denora PS, Santorelli FM, Bindoff LA. Hereditary spastic paraplegia caused by the novel mutation 1047insC in the SPG7 gene. J Neurol **255**: 1142-1144, 2008.
15. Wilkinson PA, Crosby AH, Turner C, et al. A clinical, genetic and biochemical study of *SPG7* mutations in hereditary spastic paraplegia. Brain **127**: 973-980, 2004.
16. Tsuji S, Onodera O, Goto J, Nishizawa M; Study Groupon Ataxic D. Sporadic ataxias in Japan: a population-based epidemiological study. Cerebellum **7**: 189-197, 2008.
17. Takiyama Y, Ishiura H, Shimazaki H, et al. Japan spastic paraplegia research consortium (JASPAC). Rinsho Shinkeigaku **50**: 931-934, 2010 (in Japanese, Abstract in English).
18. Majewski J, Wang Z, Lopez I, et al. A new ocular phenotype associated with an unexpected but known systemic disorder and mutation: novel use of genomic diagnostics and exome sequencing. J Med Genet **48**: 593-596, 2011.
19. Tsurusaki Y, Osaka H, Hamanoue H, et al. Rapid detection of a mutation causing X-linked leucoencephalopathy by exome sequencing. J Med Genet **48**: 606-609, 2011.
20. Bonn F, Pantakani K, Shoukier M, Langer T, Mannan AU. Functional evaluation of paraplegin mutations by a yeast complementation assay. Hum Mutat **31**: 617-621, 2010.
21. Brugman F, Scheffer H, Wokke JH, et al. *Paraplegin* mutations in sporadic adult-onset upper motor neuron syndromes. Neurology **71**: 1500-1505, 2008.
22. McDermott CJ, Dayaratne RK, Tomkins J, et al. Paraplegin gene analysis in hereditary spastic paraparesis (HSP) pedigrees in north-east England. Neurology **56**: 467-471, 2001.

CLINICAL GENETICS An International Journal of Genetics, Molecular and Personalized Medicine

Clin Genet 2013

Published by John Wiley & Sons Ltd
CLINICAL GENETICS
doi: 10.1111/cge.12215

Letter to the Editor

Whole exome sequencing revealed biallelic *IFT122* mutations in a family with CED1 and recurrent pregnancy loss

To the Editor:

Cranioectodermal dysplasia-1 (CED1), also known as Sensenbrenner syndrome (MIM 218330), is characterized by skeletal, craniofacial, and ectodermal abnormalities (1). Here, we report a family with CED1 and recurrent abortions.

I-2, 39-year-old woman, was referred to our hospital for consultation regarding recurrent abortions. Although she had one healthy boy (II-2), she suffered from two artificial abortions due to fetal hydrops at 13 weeks of gestation (II-1) and skeletal anomalies at 21 weeks of gestation (II-8), one intrauterine fetal death with hydrops at 13 weeks of gestation (II-7), and four recurrent miscarriages (II-3 at 6 weeks, II-4 at 8 weeks, II-5 at 8 weeks, and II-6 at 7 weeks) (Fig. 1a). Postmortem physical findings of II-8 included a skull deformity and blisters beside the nasal bridge due to obstetric intervention, low set ears, nuchal edema, a narrow thorax, and acromelic shortening of the limbs, posterior bowing of the lower legs and bilateral 2–3 toe syndactyly (Fig. 1b). Postmortem radiography and 3-D computed tomography showed generalized skeletal alterations which were thought to fit to CED1, though the sharp angulation of the tibiae was very unusual (Fig. 1b).

Exome sequencing was performed in I-2, II-2, and II-8 as previously described (2). We identified compound heterozygous mutations in *IFT122* in the fetal skeletal anomalies (II-8): c.1108delG (p.E370Sfs*51) in exon 11 and c.1636G>A (p.G546R) in exon 14 was inherited from his mother (Fig. 1c,d). Of note, we confirmed the same compound heterozygous mutations (c.1108delG: 2 of 29 clones, c.1636G>A: 13 of 30 clones) by capillary sequence of polymerase chain reaction (PCR) product from cloned DNA from paraffin-embedded chorionic villi (II-6) (Fig. 1e). Accordingly, c.1108delG found in II-6 and II-8 was presumed to be inherited from the father, though it was not directly confirmed.

Walczak-Sztulpa et al. reported homozygous missense mutations of *IFT122* in three patients from two consanguineous pedigrees with CED1: p.V553G in family CED-01, p.S373F in family CED-02, and compound heterozygous mutations, c.502+5G>A and p.W7C in one sporadic case, family CED-03 (1) (Fig. 1c). The four patients with *IFT122* mutations showed skeletal anomalies. We found compound heterozygous mutations in a fetus with skeletal anomalies (II-8) and the villous tissues (II-6). Clinical skeletal features of the aborted fetus (II-8) are consistent with those of the reported CED patients carrying biallelic *IFT122* mutations. Because they were found in the villous tissues (II-6) that was sequenced, biallelic *IFT122* mutations may have caused some of the recurrent abortions in this family. All four *IFT122* missense mutations (including ours) are predicted to be damaging for IFT122 function (Table 1).

CED1 belongs to a group of short rib dysplasias, including Ellis van Creveld syndrome, Jeune asphyxiating thoracic dysplasia, short rib polydactyly syndrome (SRPS) I (Saldino-Noonan), SRPS II (Majewski), SRPS III (Verma-Naumoff) and SRPS IV (Beemer-Langer) (3). The skeletal manifestation of the present fetus shared some features with other short rib dysplasias. For example, humeral bowing resembles that commonly seen in Ellis van Creveld syndrome. Severe tibial angulation was somewhat reminiscent of tibial hypoplasia in SRPS II (Majewski type). Generally, CED1 is a non-lethal disorder. However, the present family showed recurrent abortions, which can be considered as the severest phenotypes caused by biallelic *IFT122* mutations in human. Interestingly, *Ift122*-null mice show multiple developmental defects with embryonic lethality consistent with recurrent pregnancy loss in our family (4).

On the basis of the assumption that recessive mutations may cause recurrent pregnancy loss, the literatures have been carefully reviewed, but only a homozygous *HERG* mutation in a family were found to show recurrent intrauterine fetal loss (5).

In conclusion, we were able to find causative *IFT122* mutations in a non-consanguineous family with recurrent abortions. This information is useful for future counseling including preimplantatory diagnosis in this family.

Acknowledgements

We thank the family for participating in this work. We also thank Drs. Andrea Superti-Furga (Laussane, Switzerland), Jürgen Spranger (Sinzheim, Germany), and Oh Kwa Kim (Seoul, Korea) for helpful comments on the clinical phenotype. This work was supported by research grants from the Ministry of Health, Labour

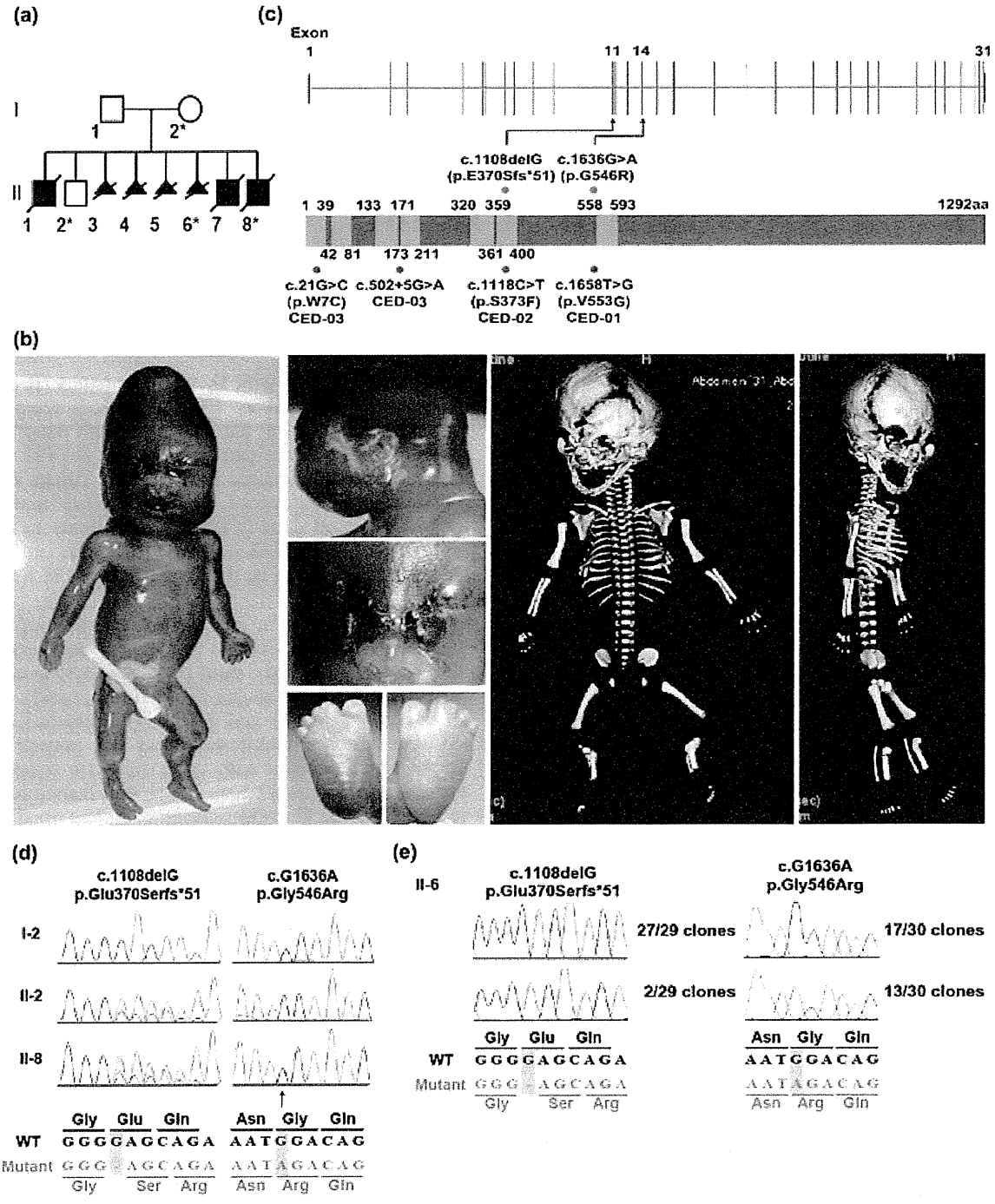

Fig. 1. Clinical finding of fetal skeletal anomalies (II-8) and genetic studies. (**a**) Familial pedigree. II-1 and II-8 were artificially terminated, II-3, II-4, II-5, II-6 and II-7 were spontaneously aborted. * DNA was available. (**b**) Clinical photographs and 3D computed tomography of II-8. (i–v) Postmortem physical findings included a skull deformity due to obstetric intervention, blisters beside the nasal bridge, low set ears, nuchal edema, a narrow thorax, and acromelic shortening of the limbs, anterior bowing of the lower legs and bilateral 2–3 toe syndactyly. (vi–vii) Postmortem 3-D computed tomography showed generalized skeletal alterations. The thorax was narrow with short ribs. The lower ribs showed a wavy appearance. The spine and ilia were normal. The long bones were not apparently short. However, the humeri were medially bowed, and the tibiae showed sharp bending at their proximal part. Ossification of the proximal and middle phalanges was defective. (**c**) The gene structure of *IFT122* (upper) and its protein structure (lower) containing seven WD40 domains (blue). Mutations found in this family and in the previous report are depicted above and below the protein, respectively. (**d**) Sequence electropherogram of family members. Compound heterozygous mutations are indicated in II-8, while healthy members (I-2 and II-2) only carry one of the two mutations. (**e**) Sequence electropherogram of the villous tissue at 7 weeks of gestation (II-6). Amplified PCR products were cloned into pCR4-TOPO vector and each clone was subjected to sequencing. Compound heterozygous mutations are indicated.

Table 1. *IFT122* mutation and their pathogenicity prediction

	Allele 1					Allele 2				
Family; Ref.	Nucleotide change	Amino acid change	SIFT	PolyPhen-2	MutationTaster	Nucleotide change	Amino acid change	SIFT	PolyPhen-2	MutationTaster
CED-01; Walczak-Sztulpa et al. (1)	c.1658T>G	p.V553G	0.00; damaging	1.000; probably damaging	1.000; disease causing	c.1658T>G	p.V553G	0.00; damaging	1.000; probably damaging	1.000; disease causing
CED-02; Walczak-Sztulpa et al. (1)	c.1118C>T	p.S373F	0.00; damaging	1.000; probably damaging	1.000; disease causing	c.1118C>T	p.S373F	0.00; damaging	1.000; probably damaging	1.000; disease causing
CED-03; Walczak-Sztulpa et al. (1)	c.21G>C	p.W7C	0.00; damaging	1.000; probably damaging	1.000; disease causing	c.502+5G>A	Splice-site change	–	–	–
This study	c.1636G>A	p.G546R	0.00; damaging	1.000; probably damaging	1.000; disease causing	c.1108delG	p.E370Sfs*51	–	–	–

and Welfare (H. S., N. Miyake, and N. Matsumoto), the Japan Science and Technology Agency (N. Matsumoto), the Strategic Research Program for Brain Sciences (N. Matsumoto) and a Grant-in-Aid for Scientific Research on Innovative Areas-(Transcription cycle)-from the Ministry of Education, Culture, Sports, Science and Technology of Japan (N. Matsumoto), a Grant-in-Aid for Scientific Research from the Japan Society for the Promotion of Science (H. S., N. Miyake, and N. Matsumoto) and a grant from the Takeda Science Foundation (N. Miyake and N. Matsumoto).

Y Tsurusaki[a]
R Yonezawa[b]
M Furuya[c]
G Nishimura[d]
RK Pooh[e]
M Nakashima[a]
H Saitsu[a]
N Miyake[a]
S Saito[b]
N Matsumoto[a]

[a]Department of Human Genetics, Yokohama City Graduate School of Medicine, Yokohama, Japan,
[b]Department of Obstetrics and Gynecology, University of Toyama, Toyama, Japan,
[c]Department of Molecular Pathology, Yokohama City Graduate School of Medicine, Yokohama, Japan,
[d]Department of Pediatric Imaging, Tokyo Metropolitan Children's Medical Center, Fuchu, Japan, and
[e]Division of Fetal Imaging Diagnosis, CRIFM Clinical Research Institute of Fetal Medicine PMC, Osaka, Japan

References

1. Walczak-Sztulpa J, Eggenschwiler J, Osborn D et al. Cranioectodermal dysplasia, sensenbrenner syndrome, is a ciliopathy caused by mutations in the IFT122 gene. Am J Hum Genet 2010: 86: 949–956.
2. Saitsu H, Nishimura T, Muramatsu K et al. De novo mutations in the autophagy gene WDR45 cause static encephalopathy of childhood with neurodegeneration in adulthood. Nat Genet 2013: 45: 445–449.
3. Eleftheriades M, Iavazzo C, Manolakos E et al. Recurrent short rib polydactyly syndrome. J Obstet Gynaecol 2013: 33: 14–16.
4. Cortellino S, Wang C, Wang B et al. Defective ciliogenesis, embryonic lethality and severe impairment of the Sonic Hedgehog pathway caused by inactivation of the mouse complex A intraflagellar transport gene Ift122/Wdr10, partially overlapping with the DNA repair gene Med1/Mbd4. Dev Biol 2009: 325: 225–237.
5. Bhuiyan ZA, Momenah TS, Gong Q et al. Recurrent intrauterine fetal loss due to near absence of HERG: clinical and functional characterization of a homozygous nonsense HERG Q1070X mutation. Heart Rhythm 2008: 5: 553–561.

Correspondence:
Naomichi Matsumoto
Department of Human Genetics
Yokohama City Graduate School of Medicine
3-9 Fukuura, Kanazawa-ku
Yokohama 236-0004
Japan
Tel.: +81 45 787 2606
Fax: +81 45 786 5219
e-mail: naomat@yokohama-cu.ac.jp

RESEARCH ARTICLE

AMERICAN JOURNAL OF medical genetics PART A

A Unique Case of De Novo 5q33.3–q34 Triplication With Uniparental Isodisomy of 5q34–qter

Atsushi Fujita,[1] Hiroshi Suzumura,[2] Mitsuko Nakashima,[1] Yoshinori Tsurusaki,[1] Hirotomo Saitsu,[1] Naoki Harada,[3] Naomichi Matsumoto,[1]* and Noriko Miyake[1]*

[1]Department of Human Genetics, Yokohama City University Graduate School of Medicine, Yokohama, Japan

[2]Department of Pediatrics, Dokkyo Medical University, Tochigi, Japan

[3]Cytogenetic Testing Group, Molecular Genetic Research and Analysis Department, Clinical Development Service Center, Mitsubishi Chemical Medience Corporation, Tokyo, Japan

Manuscript Received: 7 February 2013; Manuscript Accepted: 15 April 2013

De novo triplication together with uniparental disomy (UPD) is a rare genomic rearrangement, and, to our knowledge, co-occurrence has previously only been reported in two individuals. We encountered a patient with a suspected karyotype of 46,XX,del(5)(q33.1q33.3),dup(5)(q31.3q33.3) or (q33.1q35.1). Genetic analysis revealed tetrasomy of 5q33.3–q34 caused by de novo middle inverted triplication and uniparental isodisomy of 5q34–qter. Most clinical features in the patient were observed in previously reported cases of duplication overlapping with 5q33.3–q34, with the exception of hearing loss. The *FOXI1* gene, which causes autosomal recessive deafness (OMIM 600791, DFNB4) when mutated, was contained within the uniparental isodisomy region (5q34–qter). However, no mutations were identified following Sanger sequencing of *FOXI1*. This is the first report of a patient with de novo triplication together with uniparental isodisomy of chromosome 5q. As segmental isodisomy is a post-fertilization error, it is thought to have occurred during mitosis just after fertilization via a U-type exchange, while inverted duplication could have occurred during meiosis or mitosis. This study reaffirms that the single nucleotide polymorphism (SNP) array is a powerful tool to screen for UPD in a single experiment, especially in cases of isodisomy.

Key words: 5q; genomic rearrangement; SNP array; triplication; uniparental isodisomy

How to Cite this Article:
Fujita A, Suzumura H, Nakashima M, Tsurusaki Y, Saitsu H, Harada N, Matsumoto N, Miyake N. 2013. A unique case of de novo 5q33.3–q34 triplication with uniparental isodisomy of 5q34–qter. Am J Med Genet Part A 161A:1904–1909.

INTRODUCTION

Cytogenetically visible partial tetrasomies induced by interstitial triplications are rare genomic rearrangements, except for those that occur on chromosome 15q11–q13 [Beneteau et al., 2011]. To the best of our knowledge, triplication together with uniparental isodisomy has only been reported in two cases who presented with de novo intrachromosomal triplication at 11q23.3–q24.1 [Beneteau et al., 2011]. While there have been no reports of tetrasomy of 5q33.3–q34, the common clinical features of patients with trisomy overlapping 5q33.3–q34 are growth retardation, prominent forehead, hypertelorism, broad nasal bridge, long philtrum, thin upper lip vermilion, downturned mouth, micrognathia, low-set ears, and congenital heart defects (Table I) [Martin et al., 1985; Fryns et al., 1987; Witters et al., 1998; Rauen et al., 2001; Sanchez-Garcia et al., 2001; Martin et al., 2003].

Uniparental disomy (UPD) is defined as the condition in which two copies of a chromosomal region are inherited from only one parent. The incidence of UPD of any chromosome is estimated to be about 1:3,500 to 1:5,000 live births [Robinson, 2000; Liehr, 2010]. If imprinting genes are within the UPD region, the effect of abnormal gene transcription will appear as a phenotype. Furthermore, isodisomy has the potential to cause recessive disease [Engel, 2006]. UPD of distal 5q has previously been reported in association with three cases of spinal muscular atrophy, childhood-onset schizophrenia, and Netherton syndrome [Brzustowicz et al., 1994; Seal et al., 2006; Lin et al., 2007].

Conflict of interest: none.

*Correspondence to:
Noriko Miyake M.D., Ph.D. or Naomichi Matsumoto M.D., Ph.D., Department of Human Genetics, Yokohama City University Graduate School of Medicine, Fukuura 3–9, Kanazawa-ku, Yokohama 236-0004, Japan.
E-mails: nmiyake@yokohama-cu.ac.jp (N.Mi.) or naomat@yokohama-cu.ac.jp (N.Ma.)

Article first published online in Wiley Online Library (wileyonlinelibrary.com): 4 July 2013
DOI 10.1002/ajmg.a.36026

TABLE I. Clinical Features of Present Case and Previously Reported Patients With Pure Partial Duplications at 5q33.3–q34

	Duplication						Triplication
Case	**1**	**2**	**3**	**4**	**5**	**6**	**present case**
Gain region	q13q33	q22q33	q31.1q35.1	q31.3q33.3	q32q35.3	q33.3q35.3	q33.3q34
Origin of gain	mos [12%]	inv dup	ins(20;5)	dir dup	inv dup	inv dup	dir-inv-dir
Inheritance	De novo	mat	mat	De novo	De novo	De novo	De novo
Gestation age (weeks)	38	38	36	35	35	NA	28
Birth weight (g)	3,380	2,290	2,295	2,930	1,735	NA	607
Growth retardation	−	+	−	+	+	+	+
Microcephaly	−	+	−	+	−	NA	−
Prominent forehead	NA	NA	NA	+	+	NA	+
Hypertelorism	NA	NA	+	−	NA	+	+
Downslanting palpebral fissures	−	NA	NA	−	NA	NA	+
Strabismus	−	NA	−	−	NA	NA	−
Nasal bridge	High broad	NA	Broad	Flat	Broad	Prominent, broad	Broad
Long philtrum	+	+	NA	NA	+	+	+
Thin upper lip vermilion	+	+	NA	+	+	+	+
Downturned mouth	+	+	NA	+	NA	NA	−
Micrognathia	+	NA	NA	−	+	NA	+
Low-set ears	NA	+	−	NA	+	NA	+
Hearing loss	−	NA	−	NA	NA	NA	+
Brachydactyly	−	+	−	−	−	NA	−
Congenital heart defects	+	−	+	−	+	+	+
Reference	Rauen et al. [2001]	Martin et al. [1985]	Martin et al. [2003]	Sanchez-Garcia et al. [2001]	Fryns et al. [1987]	Witters et al. [1998]	

+, feature present; −, feature absent; NA, information not available.

Here, we present the first known patient with a de novo interstitial triplication of 5q33.3–q34 together with a segmental uniparental isodisomy of 5q34–qter. Clinical features and the mechanism of this complex chromosomal rearrangement are discussed.

MATERIALS AND METHODS

Samples

Blood was obtained from the patient and her parents after obtaining their written informed consent. DNA was extracted from blood leukocytes using QuickGene-610L (Fujifilm, Tokyo, Japan) according to the manufacturer's instructions. This study was approved by the institutional review board of Yokohama City University School of Medicine (Yokohama, Japan).

Copy Number Analysis Using Single Nucleotide Polymorphism (SNP) Arrays

Copy number analysis was performed using the CytoScanHD Array (Affymetrix, Santa Clara, CA) according to the manufacturer's protocol. Data were analyzed using Chromosome Analysis Suite software v1.2.0.225 (Affymetrix).

Quantitative PCR (qPCR)

In order to confirm the copy number changes detected by the SNP array, qPCR was performed on the Rotor-Gene Q real-time PCR cycler (Qiagen, Hilden, Germany) using the Rotor-Gene SYBR Green PCR Kit (Qiagen). The two primer sets for *NIPAL4* (NG_016626.1) and *GABRG2* (NG_009290.1) were used to amplify the tetrasomic region. *STXBP1* (NG_016623.1) and *FBN1* (NG_008805.2) genes were used as references. Primer sequences are available on request. Each sample was performed in duplicate and relative quantification analysis was performed using the relative standard curve method.

Haplotype Analysis

To determine the parental origin of the tetrasomic region of chromosome 5 in the patient, haplotyping was performed using a total of 11 microsatellite markers (*D5S424, D5S2115, D5S410, D5S412, D5S529, D5S2118, D5S422, D5S400, D5S1960, D5S2034,*

and *D5S408*). Electrophoresis of the amplicons was performed on an ABI PRISM 3130xl Genetic Analyzer (Applied Biosystems, Foster City, CA) and analyzed using Gene Mapper software v4.1.1 (Applied Biosystems).

Direct Sequencing of the Tetrasomic Region and the *FOXI1* Gene

To determine the haplotype of the tetrasomic region of the patient and to perform mutation screening of the *FOXI1* gene (NM_012188.4), *FOXI1* coding regions were sequenced with an ABI PRISM 3130xl Genetic Analyzer (Applied Biosystems) and analyzed using Sequencher software version 4.10.1 (Gene Codes Corporation, Ann Arbor, MI).

Fluorescence In Situ Hybridization (FISH)

Metaphase and interphase chromosomes of the patient and her parents were prepared from lymphoblast cell lines as previously described [Miyake et al., 2004]. Three RPCI-11 human bacterial artificial chromosome (BAC) clones were used to cover the proximal, central, and distal parts of the triplicated region: RP11-242N24 (5q33.3:156,194,944–156,365,297 bp according to the UCSC genome browser hg19), RP11-1129I9 (5q33.3:159,445,733–159,594,790 bp), and RP11-125D15 (5q34:162,601,070–162,791,863 bp), respectively.

CLINICAL REPORT

The patient is the first child of a nonconsanguineous healthy mother (G0P0, 25 years of age) and father (28 years of age). When the patient was a fetus at 18 weeks of gestation, the mother was operated on to remove an ovarian cyst. Intrauterine growth retardation was observed at 20 weeks of gestation, so the baby was born by Caesarean at 28 weeks and 5 days of gestation. Her birth weight was 607 g, and Apgar scores were 1 and 7 at 1 and 5 min, respectively. Her facial features were characterized by a prominent forehead, high hairline, hypertelorism, downslanting palpebral fissures, broad nasal bridge, anteverted nares, long philtrum, thin upper lip vermilion, micrognathia, and low-set ears. Extremities were normal.

In the neonatal intensive care unit, the patient was diagnosed with acute respiratory distress syndrome, which recovered after tracheal intubation and mechanical ventilation with surfactant administration. She was also treated with indomethacin for patent ductus arteriosus (PDA), which caused the ductus arteriosus to close the next day. After discharge at 141 days of age, developmental delay was observed. Her social smile, holding up of her head, and rolling over were recognized at 3, 8, and 9 months of corrected age, respectively, while crawling and sitting were observed at 10 and 13 months of corrected age, respectively. At 13 months of corrected age, her height was 64.7 cm (−3SD), her weight was 5,845 g (−3.2SD), and her head circumference was 41.7 cm (−2SD). She also suffered from bicuspid aortic valve stenosis and severe bilateral sensorineural hearing loss necessitating the use of hearing aids. Brain magnetic resonance imaging (MRI) findings at 129 days (1 month of corrected age) were normal. Her karyotype by Giemsa banding with trypsin (400–550 band level) in the clinical laboratory was reported as 46,XX,del(5)(q33.1q33.3),dup(5)(q31.3q33.3) or (q33.1q35.1).

RESULTS

The SNP array detected 6.5-Mb tetrasomy at 5q33.3–q34 (chr5:156,244,462–162,761,495 according to the UCSC genome browser hg19) and 18-Mb uniparental isodisomy (two copy allele with loss of heterozygosity (LOH)) at 5q34–qter (chr5: 162,761,596–180,692,321 bp) in the patient (Fig. 1A,B). The tetrasomic and UPD regions contain 39 and 159 RefSeq genes, respectively. In the tetrasomic region, three allele peaks with unusually wide spaces suggested the duplication of two haplotypes (four copies). The tetrasomic change was confirmed as de novo by qPCR (Fig. 1C).

The presence of two informative microsatellite markers *D5S412* and *D5S2118* within the tetrasomic region were indicative of biparental inheritance, whereas the other two informative microsatellite markers *D5S400* and *D5S2034* within the UPD region originated from unipaternal allele inheritance (Fig. 1D). Furthermore, direct sequencing of the four selected SNPs (rs4704896, rs1422858, rs13175902, and rs9313953) in the tetrasomic region of the patient revealed that heterozygous SNPs attained the same peak height (Fig. S1 in Supporting information online). This result supports the concept that the tetrasomic region consists of only two types of alleles, each of which derives either from the father or the mother.

To further investigate the tetrasomic region, metaphase, and interphase FISH were performed using RP11-1129I9. Three signals on one of the chromosomes 5 and one signal on the other were consistently observed in interphase nuclei (Fig. 1E). This suggested the presence of triplication in one chromosome rather than two duplications in two distinctive chromosomes. To address the orientation of each segment, dual color FISH was performed with RP11-242N24 (proximal within the segment, labeled red) and RP11-125D15 (distal, labeled green). FISH images showed a red-green (direct orientation) pattern on one of the chromosomes 5 and a red-green-red-green pattern on the other chromosome 5 with triplication (Fig. 1F). This result indicated an inverted orientation of the middle segment between two direct orientated segments (Fig. 1G). We also evaluated the possibility of mosaicism by the metaphase FISH experiment. All the checked cells (n = 100) possessed the structural abnormality, thus mosaicism was denied.

Within the UPD region were eleven genes associated with autosomal recessive diseases based on the Online Mendelian Inheritance in Man (OMIM, http://omim.org/ accessed 13 January 2013; Table SI in Supporting information online). Among these, *FOXI1* (NM_012188.4) causes hearing loss with enlarged vestibular aqueducts (DFNB4, OMIM 600791) [Yang et al., 2007], and may be related to hearing loss in the patient described here. However, Sanger sequencing of the *FOXI1* gene revealed no pathological mutations in the patient, indicating that hearing loss in this case may be caused by other factor(s). In addition, the Catalogue of Imprinted Genes (http://www.otago.ac.nz/IGC accessed 13 January 2013) indicated that no imprinting gene is known in this UPD region. Furthermore, two previously reported patients

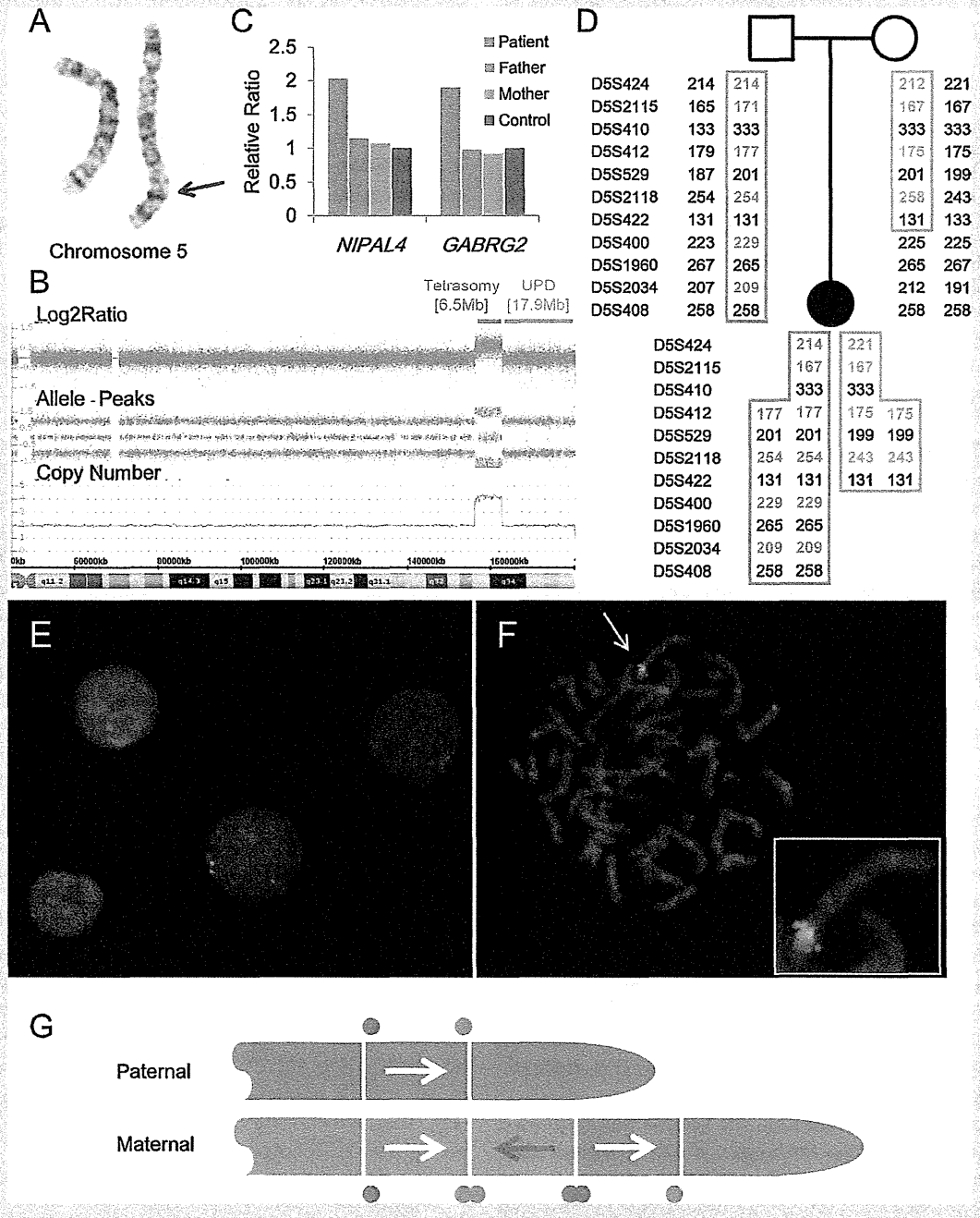

FIG. 1. Cytogenetic analysis of 5q33.3–q34 triplication and uniparental isodisomy of 5q34–qter. A: GTG image of chromosome 5 of the patient. The arrow indicates the additional segments caused by de novo triplication of 5q33.3–q34. B: The result of the SNP array. Green and blue lines indicate tetrasomic and UPD regions, respectively. C: Relative quantification of the tetrasomic region. The relative ratio in the patient was twofold that of her parents and the normal control. D: Haplotype analysis of chromosome 5. The paternal and maternal inherited haplotypes are boxed in blue and orange lines, respectively. Informative genotypes are marked in blue and orange characters. E: Interphase FISH image of the patient using the RP11-112919 probe (red) in the tetrasomic region consistently shows one isolated signal representing one copy of one allele, while the three-red-signal chain represents triplication of the other allele. F: Metaphase FISH image of the patient using the RP11-242N24 (red) and RP11-125D15 (green) probes for the proximal and distal regions of the amplified segment constantly shows red–green (bigger)–red (bigger)–green pattern on one of the chromosome 5. High magnification image of the chromosome marked by the yellow arrow is shown in the right bottom box. G: Scheme of chromosomal rearrangements in the patient. Blue and orange chromosomes indicate paternal and maternal, respectively. The middle segment of the maternal allele has an inverted orientation (red arrow) while the others are direct (white arrows). The red and green circles represent FISH signals as shown in Figure 1F.

with paternal UPD including 5q34–q35.3 did not have hearing loss [Brzustowicz et al., 1994; Seal et al., 2006], suggesting that hearing loss is unlikely to be caused by UPD.

DISCUSSION

To our knowledge, only six patients with pure partial duplication overlap with 5q33.3–q34 have been reported (Table I) [Martin et al., 1985; Fryns et al., 1987; Witters et al., 1998; Rauen et al., 2001; Sanchez-Garcia et al., 2001; Martin et al., 2003]. Common clinical features of these as well as the present case include growth retardation, prominent forehead, hypertelorism, broad nasal bridge, long philtrum, thin upper lip vermilion, downturned mouth, micrognathia, low-set ears, and congenital heart defects. Interestingly, the three patients with 5q33.3–q34 trisomy (Cases 3, 5, and 6) and the present case all have congenital heart defects and a broad nasal bridge. Most of the clinical features observed in the present case might be explained by pure partial 5q duplication, with the exception of hearing loss and other facial features such as downslanting palpebral fissures.

Using a series of molecular cytogenetic analyses, we have been able to demonstrate that the patient in the present study has de novo segmental tetrasomy consisting of an equal dosage of biparental origin with a middle inverted fragment, and terminal UPD of paternal origin. To explain this complex chromosomal rearrangement, two possible mechanisms are considered under the assumption of minimal occurrence of chromosomal breakage (Figs. S2 and 3 in Supporting information online) [Wang et al., 1999; Vialard et al., 2003].

Segmental isodisomy is caused by somatic recombination (mitosis) between paternal and maternal homologous chromosomes at the post-fertilization stage [Yamazawa et al., 2010]. In the one-step model, two U-type exchanges occur between three chromatids at mitosis just after fertilization. One U-type exchange takes place between the maternal sister chromatids "c" and "d" at the distal breakpoint region, and the other exchange takes place between homologous chromatids "b" and "c" at the proximal breakpoint region (Fig. S2 in Supporting information online). In the two-step model, inverted duplication may result from a U-type exchange between sister chromatids during maternal meiosis at the gametogenesis stage. End repair of broken fragments would then occur. After fertilization, triplication with an inverted middle repeat arises from recombination between a maternal chromosome with inverted duplication and a paternal chromosome (Fig. S3 in Supporting information online). As no cells containing different chromosome pairs existed in the proband in a form of mosaicism, they appear to have been lost (lethal); this is possible following both models (Figs. 2 and 3 in Supporting information online). The middle segment in triplication of the patient was inverted as reported previously following a U-type exchange [Wang et al., 1999; Vialard et al., 2003].

Karyotyping revealed the chromosomal aberration of the patient to be 46,XX,del(5)(q33.1q33.3),dup(5)(q31.3q33.3) or (q33.1q35.1). However, a combination of SNP array, FISH and haplotype analyses clearly revealed triplication together with paternal isodisomy. The final karyotype was interpreted as 46,XX, trp(pter→q34::q34→q33.3::q33.3→qter),arr5q33.3q34(156,244,462–162,761,495)x4,5q34qter(162,761,596–180,592,321)x2 hmz. The paternal UPD was first noticed as the LOH detected by the SNP array. Thus, following only a single experiment, the SNP array can be used for genotyping as well as the detection of copy number alterations. SNP arrays are therefore more advantageous than comparative genomic hybridization (CGH) when screening for UPD, especially isodisomy.

In conclusion, we demonstrate for the first time the de novo segmental tetrasomy of 5q33.3–q34 consisting of biparental duplication with middle inverted triplication and paternal isodisomy at 5q34–qter. We recommend that UPD be considered in future cases of tetrasomy.

ACKNOWLEDGMENTS

We thank the patient and her family for participating in this work. We also thank Ms. Y. Yamashita, S. Sugimoto, and K. Takabe for their technical assistance.

REFERENCES

Beneteau C, Landais E, Doco-Fenzy M, Gavazzi C, Philippe C, Beri-Dexheimer M, Bonnet C, Vigneron J, Walrafen P, Motte J, Leheup B, Jonveaux P. 2011. Microtriplication of 11q24.1: A highly recognisable phenotype with short stature, distinctive facial features, keratoconus, overweight, and intellectual disability. J Med Genet 48:635–639.

Brzustowicz LM, Allitto BA, Matseoane D, Theve R, Michaud L, Chatkupt S, Sugarman E, Penchaszadeh GK, Suslak L, Koenigsberger MR, Gilliam TC, Handelin BL. 1994. Paternal isodisomy for chromosome 5 in a child with spinal muscular atrophy. Am J Hum Genet 54:482–488.

Engel E. 2006. A fascination with chromosome rescue in uniparental disomy: Mendelian recessive outlaws and imprinting copyrights infringements. Eur J Hum Genet 14:1158–1169.

Fryns JP, Kleczkowska A, Borghgraef M, Raveschot J, Van den Berghe H. 1987. Distinct dysmorphic syndrome in a child with inverted distal 5q duplication. Ann Genet 30:186–188.

Liehr T. 2010. Cytogenetic contribution to uniparental disomy (UPD). Mol Cytogenet 3:8.

Lin SP, Huang SY, Tu ME, Wu YH, Lin CY, Lin HY, Lee-Chen GJ. 2007. Netherton syndrome: Mutation analysis of two Taiwanese families. Arch Dermatol Res 299:145–150.

Martin DM, Mindell MH, Kwierant CA, Glover TW, Gorski JL. 2003. Interrupted aortic arch in a child with trisomy 5q31.1q35.1 due to a maternal (20;5) balanced insertion. Am J Med Genet Part A 116A: 268–271.

Martin NJ, Cartwright DW, Harvey PJ. 1985. Duplication 5q(5q22–5q33): From an intrachromosomal insertion. Am J Med Genet 20:57–62.

Miyake N, Tonoki H, Gallego M, Harada N, Shimokawa O, Yoshiura K, Ohta T, Kishino T, Niikawa N, Matsumoto N. 2004. Phenotype–genotype correlation in two patients with 12q proximal deletion. J Hum Genet 49:282–284.

Rauen KA, Bitts SM, Li L, Golabi M, Cotter PD. 2001. Tandem duplication mosaicism: Characterization of a mosaic dup(5q) and review. Clin Genet 60:366–370.

Robinson WP. 2000. Mechanisms leading to uniparental disomy and their clinical consequences. Bioessays 22:452–459.

Sanchez-Garcia JF, de Die-Smulders CE, Weber JW, Jetten AG, Loneus WH, Hamers AJ, Engelen JJ. 2001. De novo duplication (5)(q31.3q33.3):

Report of a patient and characterization of the duplicated region using microdissection and FISH. Am J Med Genet 100:56–61.

Seal JL, Gornick MC, Gogtay N, Shaw P, Greenstein DK, Coffey M, Gochman PA, Stromberg T, Chen Z, Merriman B, Nelson SF, Brooks J, Arepalli S, Wavrant-De Vrieze F, Hardy J, Rapoport JL, Addington AM. 2006. Segmental uniparental isodisomy on 5q32–qter in a patient with childhood-onset schizophrenia. J Med Genet 43:887–892.

Vialard F, Mignon-Ravix C, Parain D, Depetris D, Portnoi MF, Moirot H, Mattei MG. 2003. Mechanism of intrachromosomal triplications 15q11–q13: A new clinical report. Am J Med Genet Part A 118A:229–234.

Wang J, Reddy KS, Wang E, Halderman L, Morgan BL, Lachman RS, Lin HJ, Cornford ME. 1999. Intrachromosomal triplication of 2q11.2–q21 in a severely malformed infant: Case report and review of triplications and their possible mechanism. Am J Med Genet 82:312–317.

Witters I, Van Buggenhout G, Moerman P, Fryns JP. 1998. Prenatal diagnosis of de novo distal 5q duplication associated with hygroma colli, fetal oedema and complex cardiopathy. Prenat Diagn 18:1304–1307.

Yamazawa K, Ogata T, Ferguson-Smith AC. 2010. Uniparental disomy and human disease: An overview. Am J Med Genet Part C 154C:329–334.

Yang T, Vidarsson H, Rodrigo-Blomqvist S, Rosengren SS, Enerback S, Smith RJ. 2007. Transcriptional control of SLC26A4 is involved in Pendred syndrome and nonsyndromic enlargement of vestibular aqueduct (DFNB4). Am J Hum Genet 80:1055–1063.

SUPPORTING INFORMATION

Additional supporting information may be found in the online version of this article at the publisher's web-site.

FIG. S1. Electropherogram for four heterozygous single nucleotide polymorphisms (SNPs) in tetrasomic region of the patient and her parents. Each heterozygous peak is of a similar height.

FIG. S2. Schematic representation of the "one-step" mechanism for de novo middle inverted triplication of biparental origin, together with paternal isodisomy. Arrowheads indicate the orientations of tetrasomic regions and dotted lines indicate breakpoint of the U-type exchange. The acentric chromosome (*) would be lost at the next cell division.

FIG. S3. Schematic representation of the "two-step" mechanism for de novo middle inverted triplication of biparental origin, together with paternal isodisomy. This model requires three chromosome breakages and two end-repairs. As mosaic cells with an absence of the 5q terminal region were not detected in the patient, they might be eliminated because of disadvantageous cell survival.

TABLE SI. Autosomal Recessive Diseases and Causative Genes at 5q34–qter